Lithium Ion–Water Clusters in Strong Electric Fields: A Quantum Chemical Study

ARTICLE *in* THE JOURNAL OF PHYSICAL CHEMISTRY A · APRIL 2015

Impact Factor: 2.69 · DOI: 10.1021/acs.jpca.5b01822 · Source: PubMed

3 AUTHORS, INCLUDING:

Christopher David Daub

Norwegian University of Science and Technol…

29 PUBLICATIONS **417** CITATIONS

SEE PROFILE

Per-Olof Åstrand

Norwegian University of Science and Technol…

106 PUBLICATIONS **2,885** CITATIONS

SEE PROFILE

THE JOURNAL OF PHYSICAL CHEMISTRY A

Article

pubs.acs.org/JPCA

Lithium Ion–Water Clusters in Strong Electric Fields: A Quantum Chemical Study

Christopher D. Daub,*[,†] Per-Olof Åstrand,[†] and Fernando Bresme[‡,†]

[†]Department of Chemistry, Norwegian University of Science and Technology (NTNU) NO-7491, Trondheim, Norway

[‡]Department of Chemistry, Imperial College London SW7 2AZ, London, United Kingdom

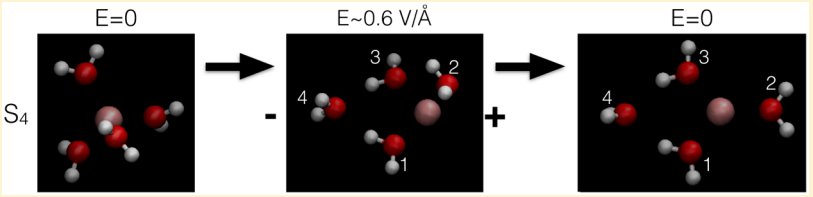

ABSTRACT: We use density functional theory to investigate the impact that strong electric fields have on the structure and energetics of small lithium ion–water clusters, $Li^+ \cdot nH_2O$, with n = 4 or 6. We find that electric field strengths of ∼0.5 V/Å are sufficient to break the symmetry of the n = 4 tetrahedral energy minimum structure, which undergoes a transformation to an asymmetric cluster consisting of three water molecules bound to lithium and one additional molecule in the second solvation shell. Interestingly, this cluster remains the global minimum configuration at field strengths ≳0.15 V/Å. The 6-coordinated cluster, $Li^+ \cdot 6H_2O$, features a similar transition to 5- and 4-coordinated clusters at field strengths of ∼0.2 and ∼0.3 V/Å, respectively, with the tetra-coordinated structure being the global minimum even in the absence of the field. Our findings are relevant to understanding the behavior of the Li^+ ion in aqueous environments under strong electric fields and in interfacial regions where field gradients are significant.

1. INTRODUCTION

Understanding the influence of electric fields on small ion clusters is of great interest for elucidating the molecular mechanisms behind a wide range of electrochemical processes. Electrospray ionization (ESI)[1−3] has been studied significantly via experiments and computer simulations in recent years.[4−8] The behavior of hydrated ions under intense electric fields is also important in electroporation of biological membranes[9−11] as well as in "bridging" transitions at interfaces separating media with different dielectric permittivities,[12] which are relevant to electrospinning processes.[13] Electrospinning is becoming increasingly important given its applicability in nanofiber manufacturing, drug delivery, and tissue engineering.[14] In the case of aqueous solutions, electric fields induce the ejection of water filaments containing ions. Good quantitative understanding of the ion solvation structure and energetics in these interfacial aqueous environments, which can differ significantly from the bulk equilibrium phase, is essential for improving the description of the molecular pathways leading to electroporation and "bridging" transitions. Such knowledge can also be of interest for assessing the importance of strong interfacial fields in biological processes, such as those occurring at the active site of enzymes.[15] More generally, the investigation of ions in low water coordination environments is relevant for understanding cluster formation in the ionosphere.[16]

Electric fields are also important at aqueous interfaces with the water/air interface being the most notable example.[17] It is well established that the reorientation of water molecules at the interface results in local interfacial fields of considerable strength. The potential drop across the water interface predicted by simulations of classical force-fields and density functional approaches are in the range −0.1 to −0.6 V[18] and −1 V,[19] respectively, although the true potential is likely much stronger. The interfacial potential predicted by classical simulations can locally be much stronger, reaching values of approximately −2 V, as reported in recent computations using methods that remove the smoothing effect of the interfacial capillary waves.[20] Modification of the interfacial potential upon the addition of salt has also been considered, showing a significant dependence on the salt concentration.[21]

Electrospray and electroporation processes involve aqueous interfaces, making it necessary to understand the behavior of the interfacial ions. Recent works have shown that small ions, particularly Li^+, feature a distinctive interfacial behavior. Computer simulations using classical models indicate that $Li^+ \cdot 4H_2O$ clusters are very stable and that they can weakly adsorb to the water surface.[20] This behavior can be modified significantly by altering the force field parameters, and small changes in the ion effective diameter can induce large modifications in the interfacial structure. These observations are important for understanding the interfacial free energy of aqueous interfaces[22,23] and the ion density enhancement at interfaces that can be inferred from simulations[24−29] and experiments.[30−32] Ion enrichment at the interface is consistent

Received: February 24, 2015
Revised: April 17, 2015
Published: April 28, 2015

DOI: 10.1021/acs.jpca.5b01822
J. Phys. Chem. A 2015, 119, 4983−4992

Table 1. Interaction Potential Energies U Between H_2O Molecules in a Dimer and Between Li^+ and One H_2O Molecule[a]

		ΔU (Li^+·H_2O)		ΔU ($2H_2O$)	
theory	basis set		BSSE		BSSE
PBE	cc-pVDZ	−183.92	−158.47	−38.68	−19.30
	cc-pVTZ	−159.76	−146.95	−28.67	−20.78
	cc-pVQZ	−153.62	−146.82	−25.29	−21.08
	cc-pV5Z	−147.45	−145.97	−22.49	−21.38
	aug-cc-pVDZ	−140.17	−139.27	−22.07	−21.39
	aug-cc-pVTZ	−144.59	−143.93	−21.32	−21.38
	aug-cc-pVQZ	−146.49	−145.45	−21.38	−21.50
	mixed, X = D	−150.04	−144.92		
	mixed, X = T	−145.81	−145.58		
	mixed, X = Q	−145.57	−145.56		
SSB-D	cc-pVDZ	−180.17	−157.59	−38.76	−17.39
	cc-pVTZ	−161.30	−148.16	−30.15	−21.17
	cc-pVQZ	−154.68	−147.43	−26.02	−21.60
	cc-pV5Z	−147.57	−146.42	−22.94	−21.85
	aug-cc-pVDZ	−142.46	−139.86	−22.63	−21.67
	aug-cc-pVTZ	−145.97	−144.87	−21.82 (−15.72[b])	−21.76
	aug-cc-pVQZ	−148.17	−146.04	−22.16	−22.13
	mixed, X = D	−150.78	−145.36		
	mixed, X = T	−146.29 (−138.24[b])	−146.05		
	mixed, X = Q	−146.27	−146.13		
CCSD	cc-pVDZ	−172.91	−152.00	−29.03	−14.73
	cc-pVTZ	−156.66	−142.83	−24.30	−17.67
	cc-pVQZ	−154.04	−145.18	−21.64	−18.91
	cc-pV5Z	−153.19		−20.56	
	Q5 fit[c]	−154.33		−20.46	
	aug-cc-pVDZ	−150.03	−137.16	−21.27	−17.86
	aug-cc-pVTZ	−150.77	−141.68	−22.64	−19.18
	aug-cc-pVQZ	−155.59	−144.75	−20.70	−19.73
	mixed, X = D	−163.82	−142.71		
	mixed, X = T	−154.92 (−153.87[d])	−144.44		
	mixed, X = Q	−154.08	−145.54		
experimental			−142.3[e]		−22.6[f]

[a]BSSE designates computations in which the basis set superposition error has been corrected as described in the text. The mixed basis sets denote computations using the cc-pV5Z basis set for Li^+ and the aug-cc-pVXZ (X = D,T,Q) basis set for H_2O. All units are in kJ/mol. [b]Substracted ZPVE. [c]Extrapolation to the basis set limit from results with cc-pVQZ and cc-pV5Z basis sets.[51] [d]CCSD(T) result. [e]From ref 67. [f]From refs 68 and 69.

with the surprising amount of bromide chemistry occurring in sea salt aerosols despite the relatively low concentration of bromide in seawater.[33] These studies show that the simple picture of an aqueous interface depleted of ions is incomplete. Instead, the current consensus is that among the simple monatomic halogens, larger anions like Br^- and I^- have a tendency to populate the interface, although the net adsorption remains negative. In ion−water clusters, even the smaller chloride anion prefers to lie closer to the surface.[34−36]

These studies illustrate the complexity of the aqueous solution interface and, by extension, of the electroporation and electrospray ionization processes discussed above. With regards to Li^+, which is the focus of our study, it is highly surprising that such a small ion can feature weak adsorption at the interface, unless the ion's hydration water plays a role in driving this effect.[20,37−39] Explicit polarizability may be important for understanding this effect, but in this case, it is the polarization of the solvent molecules at short separations from the small Li^+ ion that is crucial.[40,41] The sensitivity of the Li^+-water solvation structure can also be inferred from the analysis of extensive experimental studies, which have raised questions about the relative stability of water around Li^+.[39,42−44] In particular, it is still unclear whether the Li^+-water coordination number is closer to four or six at moderate concentrations near ∼1 M.[37,39,41,44−49]

A good understanding of the Li^+-water structure and energetics is essential to advancing the description of the nonequilibrium response of lithium-water clusters and interfacial lithium ions under electrostatic fields. We undertake this investigation in the present work as a step toward explaining the peculiar interfacial behavior of this ion and for providing microscopic information to aid in understanding of the microscopic pathways that determine electroporation and electrospray ionization processes. Our paper is structured such that we start by describing the density functional theory and ab initio methods as well as the basis sets employed. Validation of the level of theory and basis sets follows. We pursue accurate density functional theory (DFT) and ab initio calculations of the equilibrium structures and energetics of Li^+ with either four or six associated water molecules, including the effects of basis set superposition error (BSSE) to ensure the accuracy of our computations. We then discuss our results for Li^+-water clusters at equilibrium and under the influence of strong fields, paying special attention to the cluster structure and the Li^+ ion coordination number. We close with our conclusions and final remarks.

DOI: 10.1021/acs.jpca.5b01822
J. Phys. Chem. A 2015, 119, 4983−4992

Table 2. Selected Geometric Quantities from Test System Calculations[a]

		H_2O		$Li^+{\cdot}H_2O$			$2H_2O$	
theory	basis set	d_{OH}	$\angle_{HOH}$	d_{Li-O}	d_{OH}	$\angle_{HOH}$	$d_{O\cdots O}$	$\angle_{O\cdots HO}$
PBE	cc-pVDZ	0.977	101.67	1.851	0.980	104.45	1.890	166.62
	cc-pVTZ	0.970	103.53	1.840	0.973	105.30	1.920	169.34
	cc-pVQZ	0.969	103.93	1.830	0.973	105.24	1.921	170.47
	cc-pV5Z	0.969	104.16	1.830	0.973	105.23	1.925	171.93
	aug-cc-pVDZ	0.973	103.80	1.856	0.976	104.80	1.915	170.89
	aug-cc-pVTZ	0.970	104.16	1.838	0.974	105.21	1.922	170.83
	aug-cc-pVQZ	0.969	104.18	1.832	0.973	105.23	1.925	170.97
	mixed, X = D			1.826	0.976	104.84		
	mixed, X = T			1.830	0.974	105.22		
	mixed, X = Q			1.833	0.973	105.29		
SSB-D	cc-pVDZ	0.962	101.15	1.845	0.964	104.15	2.079	125.89
	cc-pVTZ	0.956	102.76	1.829	0.958	104.95	1.957	162.87
	cc-pVQZ	0.955	103.22	1.829	0.957	104.94	1.958	167.63
	cc-pV5Z	0.955	103.43	1.829	0.958	104.93	1.961	172.77
	aug-cc-pVDZ	0.958	103.05	1.849	0.960	104.52	1.959	167.18
	aug-cc-pVTZ	0.956	103.41	1.829	0.959	104.91	1.961	168.38
	aug-cc-pVQZ	0.955	103.47	1.824	0.958	104.96	1.965	168.50
	mixed, X = D			1.816	0.960	104.58		
	mixed, X = T			1.824	0.959	104.93		
	mixed, X = Q			1.825	0.957	109.97		
CCSD	cc-pVDZ	0.964	102.21	1.867	0.969	104.28	1.969	173.97
	cc-pVTZ	0.956	104.04	1.833	0.960	105.39	1.965	175.71
	cc-pVQZ	0.955	104.40	1.821	0.958	105.42	1.968	173.59
	cc-pV5Z	0.954	104.80	1.820	0.958	105.47	1.971	172.45
	aug-cc-pVDZ	0.964	104.15	1.807	0.968	104.47	1.976	172.33
	aug-cc-pVTZ	0.956	104.59	1.815	0.960	105.19	1.956	173.46
	aug-cc-pVQZ	0.955	104.73	1.802	0.959	105.41	1.963	172.27
	mixed, X = D			1.793	0.968	105.18		
	mixed, X = T			1.804	0.961	105.42		
	mixed, X = Q			1.810	0.959	105.40		

[a]All distances are in angstroms; all angles are in degrees. The mixed basis sets designate computations using the cc-pV5Z basis set for Li^+ and aug-cc-pVXZ (X = D, T, Q) basis set for H_2O.

2. COMPUTATIONAL DETAILS

For the basis sets, we use the correlation consistent basis sets of Dunning et al.,[50] cc-pVXZ and aug-cc-pVXZ. By systematically increasing the basis set as X = D, T, Q, and 5, we verify at what point we obtain converged energies with respect to the one-electron basis, and an empirical extrapolation method is used to extend these results to the basis set limit.[51] To include electron correlation, we compare the coupled-cluster with the single and double excitation (CCSD)[52,53] ab initio methodology with two different density functional theory approaches, PBE[54] and SSB-D,[55,56] the latter of which is an extension of PBE that incorporates Grimme's dispersion correction in the functional.[57,58] The SSB-D functional is thus included to investigate the contribution of dispersion interactions, which are expected to be unimportant for Li^+-water interactions but may be significant for water-water interactions in the Li^+-water clusters and under electric fields. In one of the geometries optimized by the CCSD method, we also carried out a calculation that perturbatively includes triplet excitations (CCSD(T)).[59]

BSSE was corrected for using the counterpoise correction method,[60] where energies of each component of the non-covalently bonded system are computed using the full set of basis functions of the whole system. BSSE has for a long time been recognized as a problematic issue in quantum chemical calculations of weak interactions, such as hydrogen bonding in the water dimer for example.[61−64] One cannot do geometry optimizations that correct for BSSE; therefore, the geometries are optimized without the BSSE correction, and the BSSE correction to the energy is included in subsequent single-point calculations.

An electric field can be applied to systems in a simple manner by placing a positive and negative charge ($\pm q$) equidistant from the Li^+ ion and constraining the position of the ion to be fixed in subsequent computations. The applied dipolar field strength (E) at the ion is then given by $E = 2kq/d^2$, with $k = 8.988 \times 10^9$ Nm^2/C^2, and this is the quantity we will refer to as field strength E through the remainder of the paper. Placing the charges at a distance $d = \pm 20$ Å from the ion generates an electric field from the negative to the positive ion that varies <20% within 5 Å of the ion. Charge magnitudes from ± 0.5 e to ± 15 e lead to field strengths in the 0.05−1.0 V/Å range. All computations were performed with the standard version of NWCHEM v6.3,[65] except for some molecular dynamics (MD) simulations and energy minimizations, which were done with LAMMPS.[66] The geometry optimizations were done with the DRIVER algorithm in NWCHEM and "tight" convergence criteria.

3. RESULTS

3.1. Theory and Methodological Validation. We validate our choice of basis set and level of theory for the subsequent calculations on larger clusters by systematically

DOI: 10.1021/acs.jpca.5b01822
J. Phys. Chem. A 2015, 119, 4983−4992

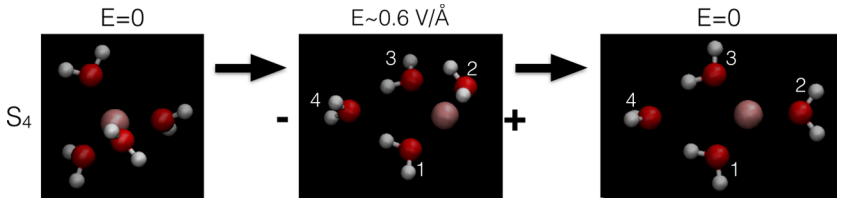

Figure 1. Snapshots of optimized geometries of the $Li^+ \cdot 4H_2O$ cluster with the SSB-D functional and the cc-pV5Z basis set for Li^+ and the aug-cc-pVTZ basis set for water. From left to right: (a) zero field, S_4 configuration; (b) field strength E = 0.58 V/Å; and (c) reoptimization after removal of the field. Labels match the molecule numbers in Table 4.

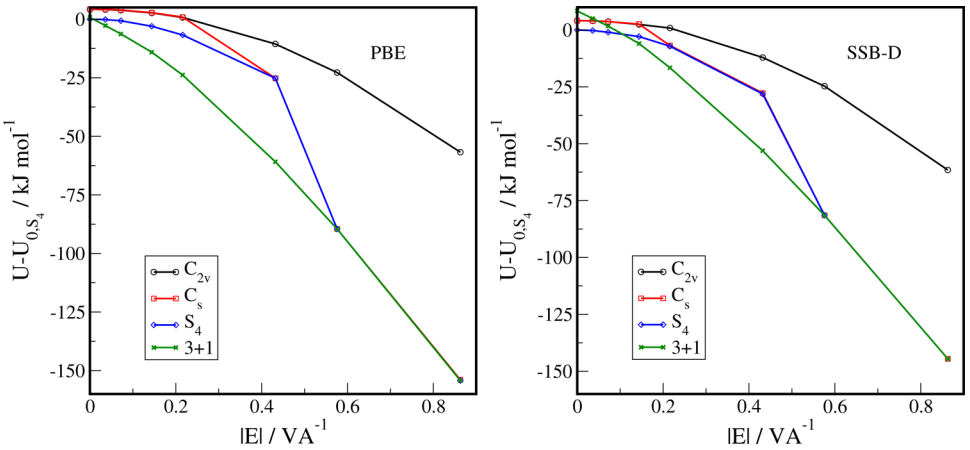

Figure 2. Plots of $U-U_{S_4}$ with the difference in binding potential energy between the optimized geometry at the indicated field strength and the global minimum geometry in zero field in the S_4 symmetry (−312.94236 E_h in the PBE calculations with the mixed basis set described in the text and −315.52698 E_h in the case of SSB-D). The legend indicates the symmetry of the initial configuration before geometry optimization. The C_{2v} and C_s configurations are distinguished by the direction of the applied electrostatic field.

testing a series of basis sets, including the effects of BSSE, using both the PBE and SSB-D density functionals as well as the CCSD method. Our test systems include monomers of both water and the Li^+ ion, water dimers,[64] and Li^+ bound to a single water molecule. Extension of the level of theory to the CCSD(T) level as well as extrapolation to the estimated basis set limit[51] led to changes of only ∼1 kJ/mol in the $Li^+ \cdot H_2O$ binding energy. All of these results are shown in Tables 1 and 2.

Our results show that the CCSD calculations are quite sensitive to BSSE, even with very large basis sets, whereas the PBE and SSB-D methods show negligible BSSE provided that the basis sets are sufficiently large. We also note a surprisingly large effect of the basis set size on the lithium ion in particular, where using the cc-pV5Z basis set was necessary to obtain well-converged results. This led us to consider mixed basis sets, where the O and H atoms are modeled with somewhat smaller basis sets. Our ultimate choices for methods and basis sets to use in the calculations on larger Li^+-water clusters are therefore the PBE and SSB-D density functional methods with the cc-pV5Z basis set on Li^+ and the aug-cc-pVTZ basis set on O and H atoms. The dispersion correction is approximately −0.6 kJ/mol for both $Li^+ \cdot H_2O$ and the water dimer. Relative to the total interaction energy of the complexes, the dispersion correction is much more important for the water dimer than for the Li^+-water complex, as expected.

We have also obtained the zero point vibrational energy (ZPVE) by computing the harmonic vibrational frequencies of the complexes and a single water molecule. The magnitude of the correction is significant in both complexes, being ∼28% of the total interaction energy in the case of the water dimer and ∼5.5% in the case of $Li^+ \cdot H_2O$.

3.2. $Li^+ \cdot 4H_2O$. Our results indicate that the global minimum for a cluster of four water molecules with Li^+ has an S_4 symmetry. This result is consistent with earlier quantum chemical computations,[37,70,71] but it does not fully agree with neutron scattering data[46] or with some classical MD results.[47] The water molecules arrange themselves in a configuration where the molecular dipoles point approximately along the Li^+-O vectors. When an electric field is applied, however, this symmetry is no longer maintained. We show in Figure 1 snapshots of the optimized configurations of the $Li^+ \cdot 4H_2O$ cluster as the electric field is varied, and in Figure 2, we plot the minimum energy obtained after geometry optimization as a function of the electric field magnitude at the Li^+ ion. The exact results vary somewhat according to the relative orientation of the electric field vector with respect to the cluster as well as the symmetry of the initial configuration. When the field is aligned with the C_{2v} axis of a cluster that initially has this symmetry, the local minimum with this symmetry is maintained up to very high field strengths in excess of 0.8 V/Å. However, if the initial cluster configuration has the global minimum S_4 symmetry, or the field is applied in a different direction, at a critical field strength of ∼0.5 V/Å, there is a breakdown in the coordination of water around the Li^+ ion and one of the waters becomes bound to one of the other water molecules instead to maximize its favorable orientation in alignment with the electric field. It is not surprising that this should occur at a high field strength, but what is more remarkable is that this asymmetric configuration with only three coordinated water molecules is actually the global minimum down to quite low field strengths. If the asymmetric configuration obtained at the high field strength is used as the starting point, and the optimization is then

DOI: 10.1021/acs.jpca.5b01822
J. Phys. Chem. A 2015, 119, 4983−4992

Table 3. Binding Energy $\Delta U_{bind} = U_{clust} - nU_{H_2O} - U_{Li^+}$ (kJ/mol) Per Water Molecule in $Li^+ \cdot nH_2O$ Clusters[a]

cluster	PBE	SSB-D	MD	from ref 71	from ref 72	from ref 37	experimental[67]
$Li^+ \cdot 3H_2O$, D_3	−121.5	−124.6		−130.6	−118.3	−117.2	−112.3
$Li^+ \cdot 3H_2O$, $N_c = 2$	−112.4	−114.5			−111.7	−107.1	
$Li^+ \cdot 4H_2O$, S_4	−107.8	−112.5 (−104.4)	−117.2	−116.4	−105.2	−105.0	−101.4
$Li^+ \cdot 4H_2O$, $N_c = 3$	−107.6	−110.4 (−101.1)	−110.9		−104.0	−102.3	
$Li^+ \cdot 6H_2O$, C_i	−83.5	−91.8			−79.6		−85.7
$Li^+ \cdot 6H_2O$, T_h	−82.3	−90.4					
$Li^+ \cdot 6H_2O$, $N_c = 5$	−85.9	−92.1					
$Li^+ \cdot 6H_2O$, $N_c = 4$	−90.1	−94.5			−90.2	−84.2	
$Li^+ \cdot 6H_2O$, $N_c = 2$	−84.6						

[a] N_c refers to the water coordination number of Li^+. All results are in zero applied electric field. Results in parentheses have subtracted the ZPVE computed with the cc-pVQZ basis set on Li^+ and the aug-cc-pVTZ basis set on O and H. The MD result is from energy minimization with classical force fields (SPC/E[74] for water, Dang's model[75] for Li^+).

converged at lower field strengths, the asymmetric configuration has a lower minimum energy above ∼0.15 V/Å with the SSB-D functional. With the PBE functional, even in the absence of an applied field, the asymmetric configuration is only 0.74 kJ/mol in energy above the four-coordinated S_4 result, and a comparatively weak field of less than 0.1 V/Å is sufficient to make this state the global minimum. Our results are consistent with previous investigations in the absence of electric field.[37,72] The binding energy per water molecule for various geometric configurations is tabulated in Table 3. We note that some of the electrostatic fields we employ here are stronger than the ∼0.35 V/Å field that caused protons to dissociate from water molecules in previous DFT based ab initio MD simulations.[73] We did not observe any dissociation events in any of our calculations, likely due to a comparatively high energy barrier that must be overcome for such an event to be observed.

A field strength of 0.15 V/Å remains quite high; however, field strengths of this size are relatively common in some contexts (e.g., in ion channels in cell membranes,[76] in membrane electroporation,[9−11] and at the tip of an atomic force microscope.[77] In fact, the electric field at an ordinary air-water interface has been calculated using the SPC/E water model and an intrinsic surface analysis to be on the order of −0.1 V/Å.[20] Our results strongly suggest that the simple picture of the $Li^+ \cdot 4H_2O$ tetrahedral structure may need to be modified, particularly under the influence of strong external fields. In particular, we have shown that the energy landscape is more complex than we expected and that there are other competing, low coordination structures that are close in energy to that of the $Li^+ \cdot 4H_2O$ cluster.

We have further computed the zero-point vibrational energy (ZPVE) of the S_4 symmetric configuration and the 3-coordinated configuration by computing the harmonic vibrational frequencies of the complexes and of a single water molecule. The ZPVE from a SSB-D calculation using the cc-pVQZ basis set on Li^+ and the aug-cc-pVTZ basis set on hydrogen and oxygen atoms is 257.4 kJ/mol, and the ZPVE of one H_2O molecule with the aug-cc-pVTZ basis set is 56.3 kJ/mol. Therefore, we determined that the total ZPVE contribution to the binding energy of the S_4 symmetric $Li^+ \cdot 4H_2O$ cluster is 32.4 or 8.1 kJ/mol per water molecule, or 7.2% of the binding energy (−112.5 kJ/mol) at the same level of theory and basis set. For comparison, the ZPVE arising from the intra- and intermolecular vibrations in the water dimer (see Table 1) is ∼6.1 kJ/mol or 28% of the total interaction energy. If the ZPVE is not considered when describing the energetics and dynamics of water exchange in and out of the solvation shell, for example, then we might expect slower residence times and stronger binding in force-field and DFT-based MD simulations. This could explain the larger coordination numbers predicted by some of the classical MD simulations of aqueous Li^+.[47] One route forward to include ZPVE corrections in MD simulations is using methods like path-integral MD[78] or centroid MD.[79] ZPVE corrections may also be implicitly included in empirical force fields parametrized against experimental data (e.g., binding energies) because many experimental determinations of binding energies also implicitly include the ZPVE.[67−69]

To investigate the ability of the classical models to reproduce the DFT results, we performed a series of energy minimizations of $Li^+ \cdot 4H_2O$ clusters using nonpolarizable empirical models with the SPC/E model[74] for water and Dang's model[75] for Li^+. These models led to a much larger difference in binding energies between the S_4 symmetry and the 3 + 1 configuration with one detached water than the DFT calculations. We completed additional classical MD simulations of the $Li^+ \cdot 4H_2O$ clusters with one detached water in the NVT ensemble at T = 300 K to estimate the relative stability of this configuration. We note that the concept of a constant temperature is inherently problematic with such a small number of particles, as the temperature features very large fluctuations. In practice, the temperature varied by ±100 K over the course of the simulations. The time at which the configuration transitioned to the S_4 symmetry varied greatly, being as low as 3 ps and as high as 92 ps over the course of ten trial runs, showing that the process is stochastic, as may be expected for an activated transition. Overall, the average transition time was 47 ± 34 ps, demonstrating that the 3 + 1 configuration with reduced symmetry can remain stable for significant time periods, and that the transformation from one structure to the other is an activated process. We recall that our computations were performed using nonpolarizable models. The similar behavior observed in our classical MD simulations and the DFT computations indicates that polarization effects do not greatly influence the relative stability of the cluster. Hence, this offers the prospect of investigating the energetics and structure of these small clusters with widely accepted nonpolarizable force fields that do not explicitly incorporate electronic degrees of freedom. This question, particularly the charge distribution in the Li^+ cluster, is discussed in more detail in the following section.

3.3. Electrostatic Potential (ESP) Surface Fitting of Partial Charges. To assess the ability of classical models to reproduce our DFT results, we have computed the ESP surface

DOI: 10.1021/acs.jpca.5b01822
J. Phys. Chem. A 2015, 119, 4983−4992

Table 4. Results of Fitting Partial Charges to the ESP at Geometries Optimized Starting from Either the S_4 or the Asymmetric 3 + 1 Configurations in the Absence of Field, Followed by the Application of the External Electric Field (see Figure 1)[a]

initial state	S_4			3 + 1			
E, VÅ^{-1}	0	0.14	0.22	0	0.14	0.22	0.43
Constrain Li^+ q = 1.0 e							
O_1	−0.863	−0.877	−0.840	−0.948	−0.962	−0.978	−0.977
H_{11}	0.428	0.427	0.411	0.447	0.474	0.475	0.473
H_{12}	0.435	0.444	0.432	0.437	0.443	0.450	0.459
O_2	"	−0.816	−0.814	−0.917	−0.905	−0.855	−0.841
H_{21}		0.406	0.405	0.452	0.449	0.430	0.430
H_{22}		0.432	0.430	0.439	0.451	0.430	0.424
O_3		−0.867	−0.845	−0.933	−0.961	−0.996	−1.058
H_{31}		0.441	0.432	0.421	0.446	0.461	0.500
H_{32}		0.423	0.412	0.455	0.473	0.481	0.491
O_4		−0.898	−0.934	−0.443	−0.685	−0.650	−0.721
H_{41}		0.444	0.458	0.300	0.384	0.371	0.410
H_{42}		0.442	0.452	0.290	0.394	0.382	0.412
RMSD	0.174	0.171	0.176	0.549	0.231	0.237	0.222
% dev.	1.42	1.39	1.42	7.06	2.08	2.10	1.89
Constrain Li^+ q = 1.0 e, All O and H Charges Equal							
O	−0.864	−0.863	−0.850	−0.931	−0.960	−0.958	−0.996
H	0.432	0.432	0.425	0.466	0.480	0.479	0.498
RMSD	0.175	0.179	0.188	0.642	0.280	0.308	0.310
% dev.	1.43	1.53	1.65	7.63	2.31	2.47	2.67

[a]Molecules are labeled as shown in Figure 1. The fourth water molecule is the detached water in the 3 + 1 configurations. RMSD denotes the root mean squared deviation between the fitted ESP and the DFT results across all grid points in kJ/mol. All data were obtained using SSB-D functionals and the mixed basis set described in the text. All charges are given in terms of the fundamental charge e = 1.602 ×10^{-19} C. Partial charges for molecules two through four in the S_4 zero field case are the same as those of the first molecule.

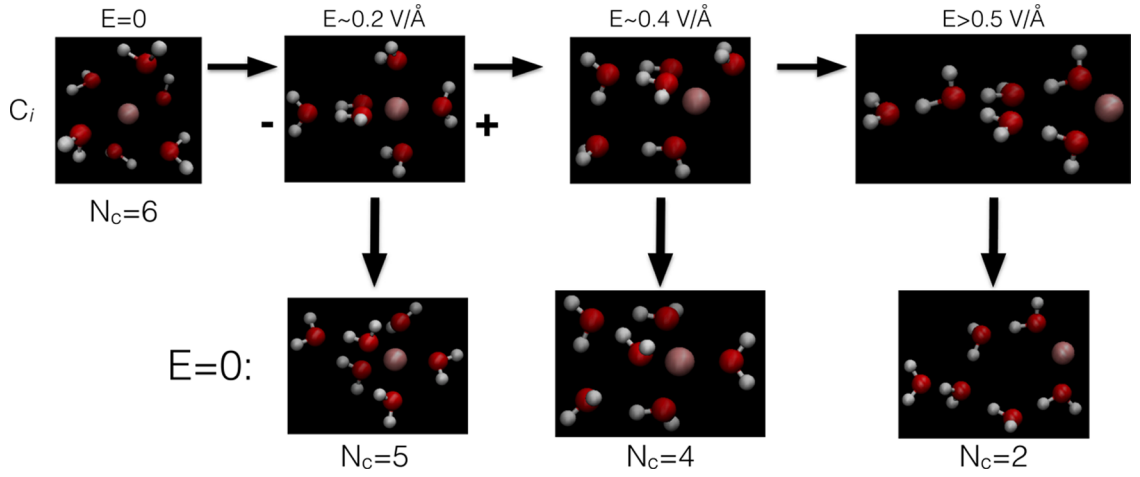

Figure 3. Snapshots of optimized geometries of the $Li^+{\cdot}6H_2O$ cluster. The top row shows configurations obtained starting from the C_i configuration as the electric field strength is increased. The bottom row shows configurations obtained after removing the applied field, starting from the respective configurations with reduced ion coordination numbers N_c. The functional and basis sets are identical to those used for the $Li^+{\cdot}4H_2O$ configurations shown in Figure 1.

and found a set of partial charges on the atomic sites that can best fit the electrostatic potential in the cluster. All of these fits were performed on the $Li^+{\cdot}4H_2O$ clusters using the default parameters in the NWCHEM ESP routine.[80] We performed these fits using two different sets of constraints: one where only the Li^+ charge was set to be 1.0 and another where, in addition, all O and H charges were each constrained to be equal as they would be in a typical classical force field. All of these results are shown in Table 4.

The largest deviations between the ESPs resulting from the partial charge fittings and the DFT results are for the 3 + 1 configuration in the absence of an external field. It is remarkable that the constrained fits (see second set of data in Table 4), which do not allow differing partial charges on atoms of the same type, do not result in a significantly worse fitting. This would suggest that fluctuating charge models[81] might not be required to describe the energetics of the asymmetric configuration, and that instead improvements should be sought from semiclassical models that include approximated atomic polarizabilities.[82]

Deviations in the asymmetric case notwithstanding, the partial charge models provide a very good description of the

DOI: 10.1021/acs.jpca.5b01822
J. Phys. Chem. A 2015, 119, 4983−4992

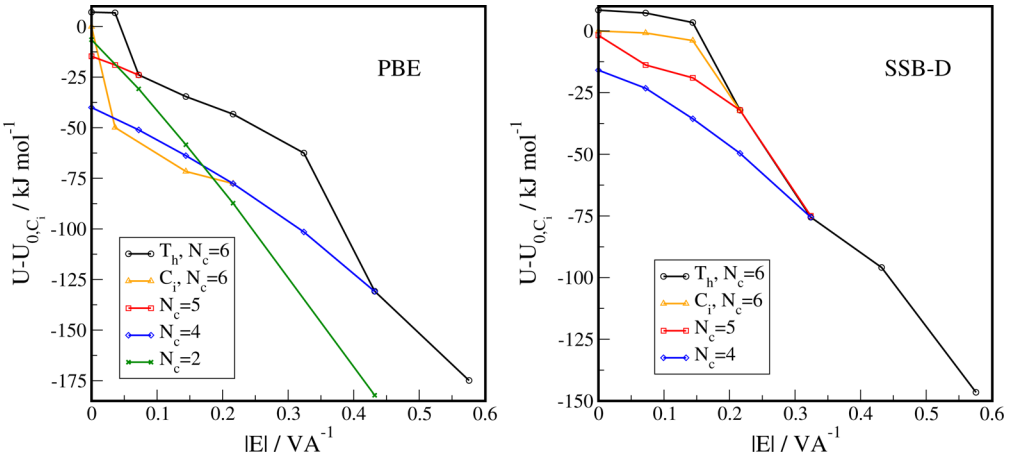

Figure 4. Plots of $U-U_{C_i}$ with the difference in potential energy between the optimized geometry at the indicated field strength and the global minimum geometry in zero field in the $N_c = 6$, C_i symmetry (−465.72962 E_h in the PBE calculations with the mixed basis set described in the text and −469.55557 E_h in the SSB-D case). The legend indicates the symmetry and/or coordination number of the initial configuration before geometry optimization. The electric field vector is colinear with one of the Li^+-O vectors in the initial C_i symmetric configuration.

ESP with mean-square deviations at each grid point ∼0.2−0.3 kJ/mol from the DFT results. The water molecules in the Li^+ clusters are found to have effective partial charges, and hence dipole moments, much greater than would be seen in an isolated water molecule, owing to the polarizing influence of the lithium ion. For comparison, we obtained results of q_O = −0.644 e and q_H = 0.322 e by fitting the ESP for the isolated water molecule with the SSB-D functional and the aug-cc-pVTZ basis set.

3.4. $Li^+·6H_2O$. We find a stable local minimum for the cluster with six water molecules in a C_i symmetry with a Li^+-water coordination number of six; however, this is not the global minimum geometry. As in the smaller four water cluster, we can alter the 6-coordinated configuration by application of an electric field. On the basis of the greater number of configurations available to the larger cluster, there is more variability in the final geometries obtained depending on factors such as the symmetry of the initial configuration and the direction of the applied field. Snapshots of a set of optimized configurations obtained in one series of calculations where the electric field was applied in a direction colinear with one of the Li^+-O vectors in the initial C_i configuration are displayed in Figure 3. Configurations with 1 or 2 detached water molecules are produced for fields in the 0.1 −0.2 V/Å range and, in the case of the PBE functional, with four detached water molecules at somewhat higher fields (∼0.5 V/Å). The elongated configurations of water molecules in the high fields with ordered dipoles are similar to those seen in simulations of small water clusters in applied fields of similar size (0.15 V/Å).[83] When these configurations are reoptimized in the absence of an applied field, we find that the configuration with $N_c = 4$ is the global minimum. The arrangement of the water molecules around the ion is nonetheless different from the one found above for the $Li^+·4H_2O$ cluster. The formation of hydrogen bonds with the two molecules not directly coodinated to Li^+ induces a reorientation of the dipoles of the water molecules that partake in the tetrahedral cluster. These dipoles do not orient along the Li^+-O vectors. This structure may be representative of an asymmetric coordination environment, such as that present at liquid-vapor interfaces. It has been recently found in classical MD simulations that lithium-water clusters adsorb at the water surface in a configuration where the clusters are oriented with one of the water molecules facing the vapor phase at the edge of the outermost interfacial layer of water.[20]

The minimum configurational energies as a function of the applied field and for different initial configurations are plotted in Figure 4 and binding energies per water molecule are reported in Table 3. As in the cluster with four water molecules, the SSB-D functional slightly reduces the preference for less symmetric or less coordinated structures versus the PBE results. However, the qualitative trends are the same. Again, we do not find evidence for dissociation of water molecules upon applying the electrostatic field.

4. CONCLUSIONS

We have peformed extensive computations of small clusters of lithium ions and water ($Li^+·nH_2O$, n = 4 or 6) in the presence of strong electrostatic fields. We have carefully tested for basis set superposition error (BSSE) and considered extrapolation to the basis set limit. We find that ab initio CCSD calculations are quite sensitive to BSSE, even with very large basis sets, whereas the PBE and SSB-D methods show negligible BSSE provided sufficiently large basis sets are used. Our DFT results for $Li^+·H_2O$ as well as the water dimer show that the combination of mixed basis sets (aug-cc-pVTZ on water atoms and cc-pV5Z on Li^+) with the SSB-D functionals provide estimates for the interaction energies with an error smaller than 2 kJ/mol with respect to the energies obtained from other high level ab initio methods.

Our computations show that the cluster of four water molecules bound to the Li^+ ion is far more stable (−113 kJ/mol per water molecule) than a cluster with 6 water molecules directly bound to the ion (−92 kJ/mol per water molecule). Hence, our results favor tetra-coordinated clusters as the stable structure rather than the value of $N_c \sim 5$ inferred from recent re-analysis of neutron scattering data.[49] The application of an electric field biases the molecular configurations around the ion toward lower coordination numbers. Of particular interest is the fact that an asymmetric configuration of three water molecules bound to the ion with the additional water molecule in a second solvation shell is actually the minimum energy configuration in a field magnitude $|E| \gtrsim 0.15$ V/Å. This is a large

DOI: 10.1021/acs.jpca.5b01822
J. Phys. Chem. A 2015, 119, 4983−4992

field strength, but such fields are relevant in interfacial systems (e.g., in electroporation[9,11] or electrospray ionization).

We have further quantified vibrational zero point energy corrections and the charge distribution in our lithium-water clusters. We found that the contribution of the zero point vibrational energy (ZPVE) to the binding energy of Li^+-water clusters is significant (8.1 kJ/mol, ∼7% of the total), albeit smaller than the ZPVE of the water dimer (6.1 kJ/mol per water molecule, ∼28% of the total). These results highlight the importance of considering zero point corrections in both force-field and ab initio molecular dynamics simulations. The atomic partial charges on the water molecules were derived by fitting the electrostatic potential surface using different charge constraint schemes, whereby the charges in the water molecules are left either as free parameters or restrained so that atoms of the same elements have the same charge. Interestingly, the constraining scheme does not have a major impact on the quality of the fit to the electrostatic potential surface, which would indicate that fluctuating charge models are not essential to describe the electrostatic environment generated by the lithium-water clusters. The fitting of the ESP of $Li^+{\cdot}4H_2O$ clusters using atomic charges is worse for asymmetric configurations, such as the 3 + 1 investigated here, which is stabilized by electric fields. This result underlines a limitation of the charge fitting approach employed here, which relies on the fitting of charges located at the atomic sites. State of the art water models (e.g., TIP4P) have highlighted the need to shift the position of the oxygen charge along the water HOH bisector. This strategy may result in a better fit of the electrostatic surface potential with point charges. We also found that the application of the electric field shifts the value of the atomic charges with respect to the charges obtained in the absence of the field. The shift is small for molecules bound directly to the Li^+ ion, ∼0.03 *e*, but can be significant, ∼0.1−0.3 *e*, for molecules not directly bound to the ion, such as the 3 + 1 configuration. Hence, accurate computations using classical models in the presence of electric fields might benefit from the consideration of polarizable force fields.

In the light of our results, it would be worthwhile to investigate the dependence of the Li^+ solvation structure, as well as other ions, on electric fields in the context of electrospray ionization experiments, particularly at the tip of the Taylor cone where the electric field is most intense.[6,84] Further work should serve to elucidate the relevance of our results to better explain the behavior of lithium ions in aqueous solutions and aqueous solution interfaces.

AUTHOR INFORMATION

Corresponding Author

*E-mail: christopher.daub@ntnu.no. Phone: (+47)98145270.

Notes

The authors declare no competing financial interest.

ACKNOWLEDGMENTS

We thank the Research Council of Norway (Project 221675) and the EPSRC (EP/J003859/1) for financial support and NOTUR (Account nn2920k) for computational resources. F.B. acknowledges an EPSRC Leadership Fellowship.

REFERENCES

(1) Dole, M.; Mack, L. L.; Hines, R. L.; Mobley, R. C.; Ferguson, L. D.; Alice, M. B. Molecular Beams of Macroions. *J. Chem. Phys.* **1968**, *49*, 2240−2249.

(2) Iribarne, J. V.; Thomson, B. A. On the evaporation of small ions from charged droplets. *J. Chem. Phys.* **1976**, *64*, 2287−2294.

(3) Fenn, J. B.; Mann, M.; Meng, C. K.; Wong, S. F.; Whitehouse, C. M. Electrospray Ionization for Mass Spectrometry of Large Biomolecules. *Science* **1989**, *246*, 64−71.

(4) Luedtke, W. D.; Landmann, U.; Chiu, Y.-H.; Levandier, D. J.; Dressler, R. A.; Sok, S.; Gordon, M. S. Nanojets, Electrospray, and Ion Field Evaporation: Molecular Dynamics Simulations and Laboratory Experiments. *J. Phys. Chem. A* **2008**, *112*, 9628−9649.

(5) Daub, C. D.; Cann, N. M. How Are Completely Desolvated Ions Produced in Electrospray Ionization: Insights from Molecular Dynamics Simulations. *Anal. Chem.* **2011**, *83*, 22393−22399.

(6) Wu, X.; Oleschuk, R. D.; Cann, N. M. Characterization of microstructured fibre emitters: in pursuit of improved nano electrospray ionization performance. *Analyst* **2012**, *137*, 4150−4161.

(7) Konermann, L.; McAllister, R. G.; Metwally, H. Molecular Dynamics Simulations of the Electrospray Process: Formation of NaCl Clusters via the Charged Residue Mechanism. *J. Phys. Chem. B* **2014**, *118*, 12025−12033.

(8) Consta, S.; Oh, M. I.; Soltani, S. Advances in the theoretical and molecular simulation studies of the ion chemistry in droplets. *Int. J. Mass Spectrom.* **2015**, *377*, 557−567.

(9) Tieleman, D. P.; Leontiadou, H.; Mark, A. E.; Marrink, S.-J. Simulation of Pore Formation in Lipid Bilayers by Mechanical Stress and Electric Fields. *J. Am. Chem. Soc.* **2003**, *125*, 6382−6383.

(10) Tarek, M. Membrane Electroporation: A Molecular Dynamics Simulation. *Biophys. J.* **2005**, *88*, 4045−4053.

(11) Delemotte, L.; Tarek, M. Molecular Dynamics Simulations of Lipid Membrane Electroporation. *J. Membr. Biol.* **2012**, *245*, 531−543.

(12) Woisetschläger, J.; Wexler, A. D.; Holler, G.; Eisenhut, M.; Gatterer, K.; Fuchs, E. C. Horizontal bridges in polar dielectric liquids. *Exp. Fluids* **2012**, *52*, 193−205.

(13) Jirsák, J.; Moucka, F.; Nezbeda, I. Insight into Electrospinning via Molecular Simulations. *Ind. Eng. Chem. Res.* **2014**, *53*, 8257−8264.

(14) Sill, T. J.; von Recum, H. A. Electro spinning: Applications in drug delivery and tissue engineering. *Biomaterials* **2008**, *29*, 1989−2006.

(15) Suydam, I. T.; Snow, C. D.; Pande, V. S.; Boxer, S. G. Electric Fields at the Active Site of an Enzyme: Direct Comparison of Experiment with Theory. *Science* **2006**, *313*, 200−204.

(16) Ferguson, E. E. Mass Spectrometry in Ionospheric Research. *Mass Spectrom. Rev.* **2007**, *26*, 142−149.

(17) Saykally, R. J. Two sides of the acid-base story. *Nat. Chem.* **2013**, *5*, 82−84.

(18) Sokhan, V.; Tildesley, D. J. The free surface of water: molecular orientation, surface potential and nonlinear susceptibility. *Mol. Phys.* **1997**, *92*, 625−640.

(19) Bresme, F.; Artacho, E. Electronic structure computations of Newton Black Films. *J. Mater. Chem.* **2010**, *20*, 10351−10358.

(20) Bresme, F.; Chacón, E.; Tarazona, P.; Wynveen, A. The structure of ionic aqueous solutions at interfaces: An intrinsic structure analysis. *J. Chem. Phys.* **2012**, *137*, 114706.

(21) Wick, C. D.; Dang, L. X.; Jungwirth, P. Simulated surface potentials at the vapor-water interface for the KCl aqueous electrolyte solution. *J. Chem. Phys.* **2006**, *125*, 024706.

(22) Heydweiller, A. Über physikalische Eigenschaften von Lösungen in ihrem Zusammenhang. II. Oberflächenspannung und elektrisches Leitvermögen wässeriger Salzlösungen. *Ann. Phys. (Berlin)* **1910**, *338*, 145−185.

(23) Jones, G.; Ray, W. A. The Surface Tension of Solutions of Electrolytes as a Function of the Concentration. I. A Differential Method for Measuring Relative Surface Tension. *J. Am. Chem. Soc.* **1937**, *59*, 187−198.

(24) Jungwirth, P.; Tobias, D. J. Molecular Structure of Salt Solutions: A New View of the Interface with Implications for Heterogeneous Atmospheric Chemistry. *J. Phys. Chem. B* **2001**, *105*, 10468−10472.

DOI: 10.1021/acs.jpca.5b01822
J. Phys. Chem. A 2015, 119, 4983−4992

(25) Dang, L. X.; Chang, T.-M. Molecular Mechanism of Ion Binding to the Liquid/Vapor Interface of Water. *J. Phys. Chem. B* **2002**, *106*, 235−238.
(26) Jungwirth, P. Ions at aqueous interfaces. *Faraday Discuss.* **2009**, *141*, 9−30.
(27) Caleman, C.; Hub, J. S.; van Maaren, P. J.; van der Spoel, D. Atomistic simulation of ion solvation in water explains surface preference of halides. *Proc. Natl. Acad. Sci.* **2011**, *108*, 6838−6842.
(28) Bauer, B. A.; Ou, S.; Patel, S. Solvation structure and energetics of single ions at the aqueous liquid-vapor interface. *Chem. Phys. Lett.* **2012**, *527*, 22−26.
(29) Tobias, D. J.; Stern, A. C.; Baer, M. D.; Levin, Y.; Mundy, C. J. Simulation and Theory of Ions at Atmospherically Relevant Aqueous Liquid-Air Interfaces. *Annu. Rev. Phys. Chem.* **2013**, *64*, 339−359.
(30) Liu, D.; Ma, G.; Levering, L. M.; Allen, H. C. Vibrational Spectroscopy of Aqueous Sodium Halide Solutions and Air-Liquid Interfaces: Observation of Increased Interfacial Depth. *J. Phys. Chem. B* **2004**, *108*, 2252−2260.
(31) Otten, D. E.; Shaffer, P. R.; Geissler, P. L.; Saykally, R. J. Elucidating the mechanism of selective ion adsorption to the liquid water surface. *Proc. Nat. Acad. Sci. U.S.A.* **2012**, *109*, 701−705.
(32) Petersen, P. B.; Saykally, R. J. On the Nature of Ions at the Liquid Water Surface. *Annu. Rev. Phys. Chem.* **2006**, *57*, 333−364.
(33) Knipping, E. M.; Lakin, M. J.; Foster, K. L.; Jungwirth, P.; Tobias, D. J.; Gerber, R. B.; Dabdub, D.; Finlayson-Pitts, B. J. Experiments and Simulations of Ion-Enhanced Interfacial Chemistry on Aqueous NaCl Aerosols. *Science* **2000**, *288*, 301−306.
(34) Perera, L.; Berkowitz, M. L. Many-body effects in molecular dynamics simulations of $Na^+(H_2O)_n$ and $Cl^-(H_2O)_n$ clusters. *J. Chem. Phys.* **1991**, *95*, 1954−1963.
(35) Stuart, S. J.; Berne, B. J. Effects of Polarizability on the Hydration of the Chloride Ion. *J. Phys. Chem.* **1996**, *100*, 11934−11943.
(36) Koch, D. M.; Peslherbe, G. H. On the transition from surface to interior solvation in iodide-water clusters. *Chem. Phys. Lett.* **2002**, *359*, 381−389.
(37) San-Román, M. L.; Carrillo-Tripp, M.; Saint-Martin, H.; Hernández-Cobos, J.; Ortega-Blake, I. A theoretical study of the hydration of Li^+ by Monte Carlo simulations with refined ab initio based model potentials. *Theor. Chem. Acc.* **2006**, *115*, 117−189.
(38) Wynveen, A.; Bresme, F. Properties of alkali-halide salt solutions about polarizable nanoparticle solutes for different ion models. *J. Chem. Phys.* **2010**, *133*, 144706.
(39) Zeng, Y.; Wang, C.; Zhang, X.; Ju, S. Solvation structure and dynamics of Li^+ ion in liquid water, methanol and ethanol: A comparison study. *Chem. Phys.* **2014**, *433*, 89−97.
(40) Masia, M.; Probst, M.; Rey, R. On the performance of molecular polarization methods. II. Water and carbon tetrachloride close to a cation. *J. Chem. Phys.* **2005**, *123*, 164505.
(41) Pejov, L.; Spångberg, D.; Hermansson, K. Using MD snapshots in ab initio and DFT calculations: OH vibrations in the first hydration shell around $Li^+(aq)$. *J. Phys. Chem. A* **2005**, *109*, 5144−5152.
(42) Spångberg, D.; Rey, R.; Hynes, J. T.; Hermansson, K. Rate and Mechanisms for Water Exchange around $Li^+(aq)$ from MD Simulations. *J. Phys. Chem. B* **2003**, *107*, 4470−4477.
(43) Møller, K. B.; Rey, R.; Masia, M.; Hynes, J. T. On the coupling between molecular diffusion and solvation shell exchange. *J. Chem. Phys.* **2005**, *122*, 114508.
(44) Wilkins, D. M.; Manolopoulos, D. E.; Dang, L. X. Nuclear quantum effects in water exchange around lithium and fluoride ions. *J. Chem. Phys.* **2015**, *142*, 064509.
(45) Chandrasekhar, J.; Spellmeyer, D. C.; Jorgensen, W. L. Energy component analysis for dilute aqueous solutions of Li^+, Na^+, F^-, and Cl^- ions. *J. Am. Chem. Soc.* **1984**, *106*, 903−910.
(46) Howell, I.; Nielson, G. W. Li^+ hydration in concentrated aqueous solution. *J. Phys.: Condens. Matter* **1996**, *8*, 4455−4463.
(47) Egorov, A. V.; Komolkin, A. V.; Chizhik, V. I.; Yushmanov, P. V.; Lyubartsev, A. P.; Laaksonen, A. Temperature and Concentration Effects on Li^+-Ion Hydration. A Molecular Dynamics Simulation Study. *J. Phys. Chem. B* **2003**, *107*, 3234−3242.
(48) Öhrn, A.; Karlström, G. A combined quantum chemical statistical mechanical simulation of the hydration of Li^+, Na^+, F^-, and Cl^-. *J. Phys. Chem. B* **2004**, *108*, 8452−8459.
(49) Mason, P. E.; Ansell, S.; Neilson, G. W.; Rempe, S. B. Neutron Scattering Studies of the Hydration Structure of Li^+. *J. Phys. Chem. B* **2015**, *119*, 2003−2009.
(50) Woon, D. E.; Dunning, T. H., Jr. Gaussian basis sets for use in correlated molecular molecular calculations. IV. Calculation of static electrical response properties. *J. Chem. Phys.* **1994**, *100*, 2975−2988.
(51) Halkier, A.; Helgaker, T.; Jørgensen, P.; Klopper, W.; Koch, H.; Olsen, J.; Wilson, A. K. Basis-set convergence in correlated calculations on Ne, N_2, and H_2O. *Chem. Phys. Lett.* **1998**, *286*, 243−252.
(52) Rendell, A. P.; Lee, T. J.; Komornicki, A.; Wilson, S. Evaluation of the contribution from triply excited intermediates to the fourth-order perturbation theory energy on Intel distributed memory supercomputers. *Theor. Chem. Acc.* **1993**, *84*, 271−287.
(53) Kobayashi, R.; Rendell, A. P. A direct coupled cluster algorithm for massively parallel computers. *Chem. Phys. Lett.* **1997**, *265*, 1−11.
(54) Perdew, J. P.; Burke, K.; Ernzerhof, M. Generalized gradient approximation made simple. *Phys. Rev. Lett.* **1996**, *77*, 3865−3868.
(55) Swart, M.; Solà, M.; Bickelhaupt, F. M. Switching between OPTX and PBE exchange functionals. *J. Comput. Methods Sci. Eng.* **2009**, *9*, 69−77.
(56) Swart, M.; Solà, M.; Bickelhaupt, F. M. A new all-round density functional based on spin states and S(N)2 barriers. *J. Chem. Phys.* **2009**, *131*, 094103.
(57) Grimme, S. Accurate description of van der Waals complexes by density functional theory including empirical corrections. *J. Comput. Chem.* **2004**, *25*, 1463−1473.
(58) Grimme, S. Semiempirical GGA-type density functional constructed with a long-range dispersion correction. *J. Comput. Chem.* **2006**, *27*, 1787−1799.
(59) Raghavachari, K.; Trucks, G. W.; Pople, J. A.; Head-Gordon, M. A fifth-order perturbation comparison of electron correlation theories. *Chem. Phys. Lett.* **1989**, *157*, 479−483.
(60) Boys, S. F.; Bernardi, F. The calculation of small molecular interactions by the differences of separate total energies. Some procedures with reduced errors. *Mol. Phys.* **1970**, *19*, 553−566.
(61) Newton, M. D.; Kestner, N. R. The water dimer: Theory versus experiment. *Chem. Phys. Lett.* **1983**, *94*, 198−201.
(62) Szalewicz, K.; Cole, S. J.; Kołos, W.; Bartlett, R. J. A theoretical study of the water dimer interaction. *J. Chem. Phys.* **1988**, *89*, 3662−3673.
(63) Åstrand, P.-O.; Wallqvist, A.; Karlström, G. On the basis set superposition error in the evaluation of water dimer interactions. *J. Phys. Chem.* **1991**, *95*, 6395−6396.
(64) Halkier, A.; Koch, H.; Jørgensen, P.; Christiansen, O.; Nielsen, I. M. B.; Helgaker, T. A systematic ab initio study of the water dimer in hierarchies of basis sets and correlation models. *Theor. Chem. Acc.* **1997**, *97*, 150−157.
(65) Valiev, M.; et al. NWChem: A comprehensive and scalable open-source solution for large scale molecular simulations. *Comput. Phys. Commun.* **2010**, *181*, 1477−1489.
(66) Plimpton, S. J. Fast Parallel Algorithms for Short-Range Molecular Dynamics. *J. Comput. Phys.* **1995**, *117*, 1−19.
(67) Džidić, I.; Kebarle, P. Hydration of the Alkali Ions in the Gas Phase. Enthalpies and Entropies of Reactions $M^+(H_2O)_{n-1} + H_2O = M^+(H_2O)_n$. *J. Phys. Chem.* **1970**, *74*, 1466−1474.
(68) Curtiss, L. A.; Frurip, D. J.; Blander, M. Studies of molecular association in H_2O and D_2O vapors by measurement of thermal conductivity. *J. Chem. Phys.* **1979**, *71*, 2703−2711.
(69) Reimers, J. R.; Watts, R. O.; Klein, M. L. Intermolecular potential functions and the properties of water. *Chem. Phys.* **1982**, *64*, 95−114.
(70) Feller, D.; Glendening, E. D.; Woon, D. E.; Feyerisen, M. W. An extended basis set ab initio study of alkali metal cation-water clusters. *J. Chem. Phys.* **1995**, *103*, 3526−3542.

DOI: 10.1021/acs.jpca.5b01822
J. Phys. Chem. A 2015, 119, 4983−4992

(71) Pye, C. C.; Rudolph, W.; Poirier, R. A. An ab Initio Investigation of Lithium Ion Hydration. *J. Phys. Chem.* **1996**, *100*, 601−605.
(72) Li, X.; Yang, Z.-Z. Study of Lithium Cation in Water Clusters: Based on Atom-Bond Electronegativity Equalization Method Fused into Molecular Mechanics. *J. Phys. Chem. A* **2005**, *109*, 4102−4111.
(73) Saitta, A. M.; Saija, F.; Gianquinta, P. V. Ab Initio Molecular Dynamics Study of Dissociation of Water under an Electric Field. *Phys. Rev. Lett.* **2012**, *108*, 207801.
(74) Berendsen, H. J. C.; Grigera, J. R.; Straatsma, T. P. The Missing Term In Effective Pair Potentials. *J. Phys. Chem.* **1987**, *91*, 6269−6271.
(75) Dang, L. X. Development of nonadditive intermolecular potentials using molecular dynamics: Solvation of Li^+ and F^- ions in polarizable water. *J. Chem. Phys.* **1992**, *96*, 6970−6977.
(76) Philippsen, A.; Im, W.; Engel, A.; Schimer, T.; Roux, B.; Müller, D. J. Imaging the Electrostatic Potential of Transmembrane Channels: Atomic Probe Microscopy of OmpF Porin. *Biophys. J.* **2002**, *82*, 1667−1676.
(77) Guan, L.; Qi, G.; Liu, S.; Zhang, H.; Zhang, Z.; Yang, Y.; Wang, C. Nanoscale Electrowetting Effects Studied by Atomic Force Microscopy. *J. Phys. Chem. C* **2009**, *113*, 661−665.
(78) Berne, B. J.; Thirumalai, D. On the Simulation of Quantum-Systems - Path Integral Methods. *Annu. Rev. Phys. Chem.* **1986**, *37*, 401−424.
(79) Pavese, M.; Berard, D. R.; Voth, G. A. Ab initio centroid molecular dynamics: a fully quantum method for condensed-phase dynamics simulations. *Chem. Phys. Lett.* **1999**, *300*, 93−98.
(80) Chipot, C.; Maigret, B.; Rivail, J.-L.; Scheraga, H. A. Modeling Amino Acid Side Chains. 1. Determination of Net Atomic Charges from ab Initio Self-Consistent-Field Molecular Electrostatic Properties. *J. Phys. Chem.* **1992**, *96*, 10276−10284.
(81) Rick, S. W.; Stuart, S. J.; Berne, B. J. Dynamical fluctuating charge force fields: Application to liquid water. *J. Chem. Phys.* **1994**, *101*, 6141−6156.
(82) Åstrand, P.-O.; Linse, P.; Karlström, G. Molecular dynamics study of water adopting a potential function with explicit atomic dipole moments and anisotropic polarizabilities. *Chem. Phys.* **1995**, *191*, 195−202.
(83) Vegiri, A. Reorientational relaxation and rotational-translational coupling in water clusters in a d.c. external electric field. *J. Mol. Liq.* **2004**, *110*, 155−168.
(84) Taylor, G. Disintegration of Water Drops in an Electric Field. *Proc. R. Soc. A* **1964**, *280*, 383−397.

DOI: 10.1021/acs.jpca.5b01822
J. Phys. Chem. A 2015, 119, 4983−4992